JOURNAL OF MATERIALS SCIENCE 20 (1985) 3501–3514

Removal of inclusions from steel melts by filtration

D. APELIAN, R. MUTHARASAN*, S. ALI
*Department of Materials Engineering, and *Department of Chemical Engineering, Drexel University, Philadelphia, Pennsylvania 19104, USA*

The removal of alumina inclusions from steel melts is characterized both qualitatively and quantitatively. Two specific types of filters have been used in this investigation: (1) tabular alumina having 0.2 to 0.5 cm particle size, and (2) extruded cellular monolithic alumina having 400 square cells per in^2. The starting steel melts contained alumina inclusions of the order of 1 to 5 μm in size. Both chemical analyses and quantitative metallography of samples before and after filtration were carried out; in the latter, volume fraction and the size distribution of the inclusions were evaluated. It was found that alumina inclusions greater than 2.5 μm were completely removed by filtration and those smaller than 2.5 μm were substantially reduced in terms of number of inclusions per mm^2. A good correlation has been found between filtration performance data evaluated by quantitative metallographic techniques and those evaluated by chemical analysis.

1. Introduction

The demand for clean steels is forcing steelmaking metallurgy beyond the decimal point. Applications such as steel beverage containers are dictating levels of non-metallic inclusions once thought impossible to attain. It is well established that the size, type and distribution of non-metallic inclusions in steels dramatically affects the mechanical properties of the cast product [1–4]. Steel refining can be carried out both physically and chemically; in the recent past a great deal has been published on ladle refining [5–7] where chemical refining is the predominant mode. In contrast, removal of inclusions from steel by filtration is a physical refining process.

The non-metallic inclusions which need to be removed from steel melts are oxides, carbides, nitrides and sulphides. These impurities may be characterized as: (1) exogenous inclusions, e.g. reaction products as a result of the furnace atmosphere, refractory particles suspended in the melt, and (2) endogenous inclusions (reaction products resulting from the deoxidation of the steel melt) such as alumina or hercynite. Steel filtration has been successfully carried out to remove alumina inclusions (formed *in situ*) from steel melts [8]. The objective of this paper is to show that quantitative metallographic analysis can be used to characterize the level of steel cleanliness by filtration processing. Filtration performance data based on quantitative chemical analysis are compared and correlated to those based on quantitative metallographic techniques.

2. Metal filtration technology and principles

The fact that tundish nozzles in continuous casting block due to the deposition of alumina inclusions is reason enough to give credence to the thesis that filtration is a viable refining process to produce clean steels. In steel filtration, the melt containing inclusions flows past the grains or channels of the filter medium and inclusions deposit on to the surface of the filter. The deposited inclusions rapidly sinter to the filter surface and act as new filter sites for further capture of inclusions. Although inclusion removal by filtration is termed physical refining,

0022–2461/85 $03.00 + .12 © *1985 Chapman and Hall Ltd.*

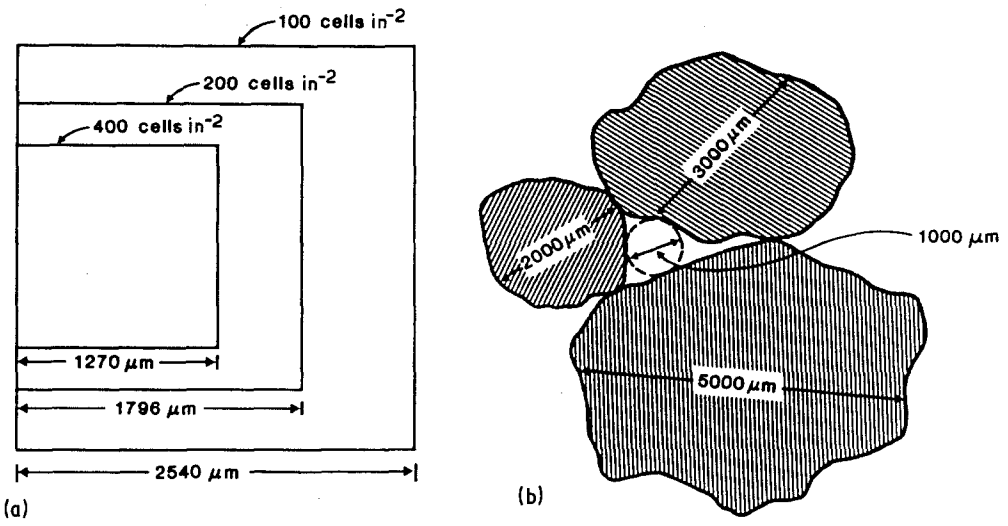

Figure 1 Schematic representation of filter pore size and inclusion size: (a) monolithic filter; (b) tabular filter.

it should be noted that the inclusions which are being captured are about 200 to 300 times smaller than the typical pore opening present in the filter and hence inclusion removal is not due to pure physical separation. Fig. 1 is a schematic portrayal of the size of the inclusions and the filter pores, which are several orders of magnitude larger than the inclusions. Inclusion removal from steel melts can be visualized as consisting of two primary serial steps. First, the inclusion is transported to the filter surface by local fluid dynamics. The second step consists of adherence or sintering of the inclusion to the filter surface due to secondary forces [9].

High performance filter media have been developed for filtration of steel melts. Specifically, there are three different types of media: tabular, monolithic and foam. In this study only the tabular and monolithic filters are evaluated. The tabular alumina filter consists of small granules of alumina pieces packed within a filter box (alumina crucible), and the melt is passed through this deep bed. The monolithic alumina filter is an extruded product which can be inserted in the ingate of the tundish. The multicellular nature of this filter not only provides a medium for filtration but also acts as a flow laminarizer and reduces melt splashing. Fig. 2 shows these filter media.

3. Filtration experiments

Steel containing 0.012 wt % C, 0.04 wt % Ni and 12 to 20 ppm oxygen was used as the starting charge material. The oxygen content of the melt was brought up to the level of about 400 to 600 ppm by the addition of Fe_2O_3 powder to the

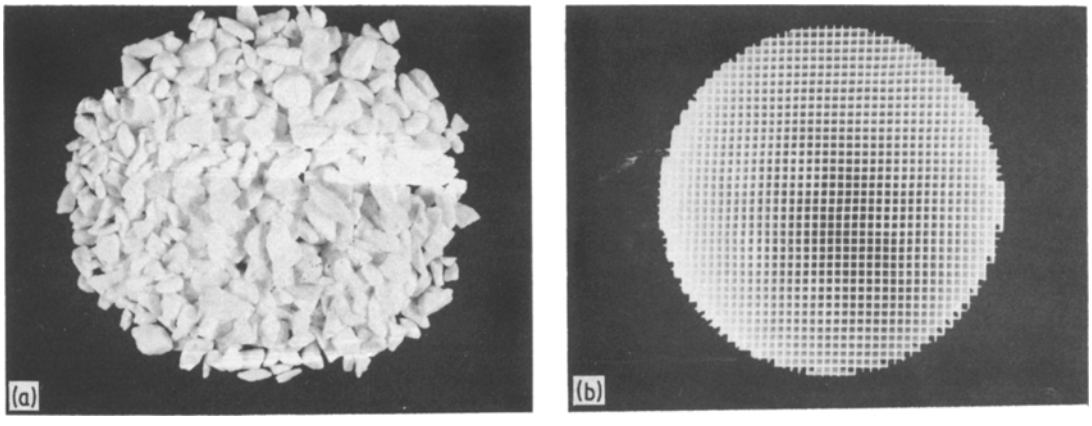

Figure 2 Photographs showing (a) the unused tabular and (b) the monolithic alumina filters.

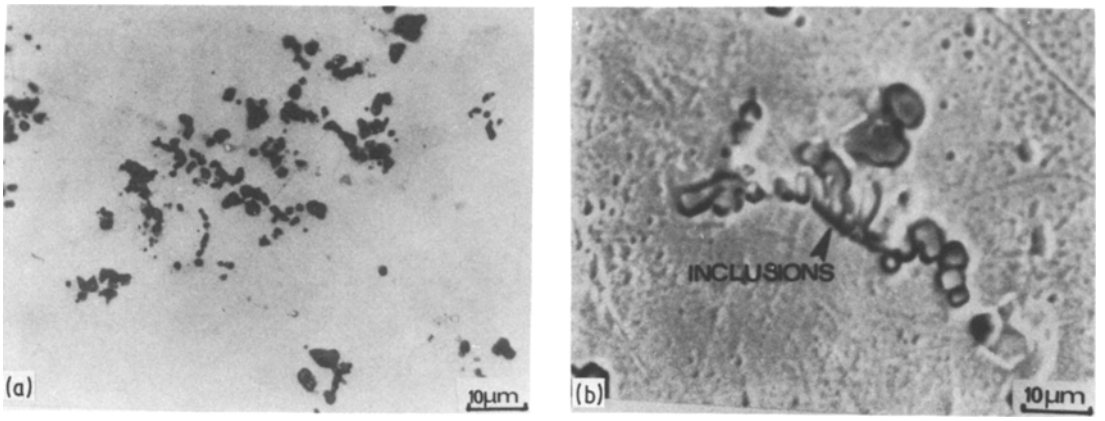

Figure 3 (a) Optical micrograph and (b) scanning electron micrograph showing the presence of alumina inclusions in filtered steel melts.

charge. Subsequently, the melt was deoxidized *in situ* by the addition of high purity aluminium wire. Representative micrographs of the deoxidation product, the alumina inclusions, are shown in Fig. 3. Clustering of the inclusions was not observed and the individual inclusions are in the size range of 1 to 5 μm.

Different filter heights were used: the tabular alumina granules (0.2 to 0.5 cm size) were packed in an alumina crucible to lengths of 5, 10 and 15 cm; monolithic filters of 5 and 10 cm height were used which were cemented in place in an alumina tube, see Fig. 4.

The filtration apparatus used in this study is shown in Fig. 5. There are two sections to the assembly – the upper section consists of a stainless steel dome (55 cm i.d. and 75 cm high) which houses the induction coil and the crucible containing the melt and the filter. The lower section houses the melt receiving crucible made of stainless steel (50.8 cm i.d. and 29.2 cm high with a 2° taper). The receiving crucible is water-cooled from the bottom end and rests on a load cell which is attached to a strip chart recorder and measures the melt velocity during filtration.

In this set-up the filter and the steel charge (1.5 to 2 kg) were simultaneously heated by a 1.5 cm thick cylindrical graphite susceptor via induction heating (10 kW and 40 kHz). A stopper rod arrangement was used to control melt infiltration into the filter. During a given run, the temperature along the surface of the crucible was

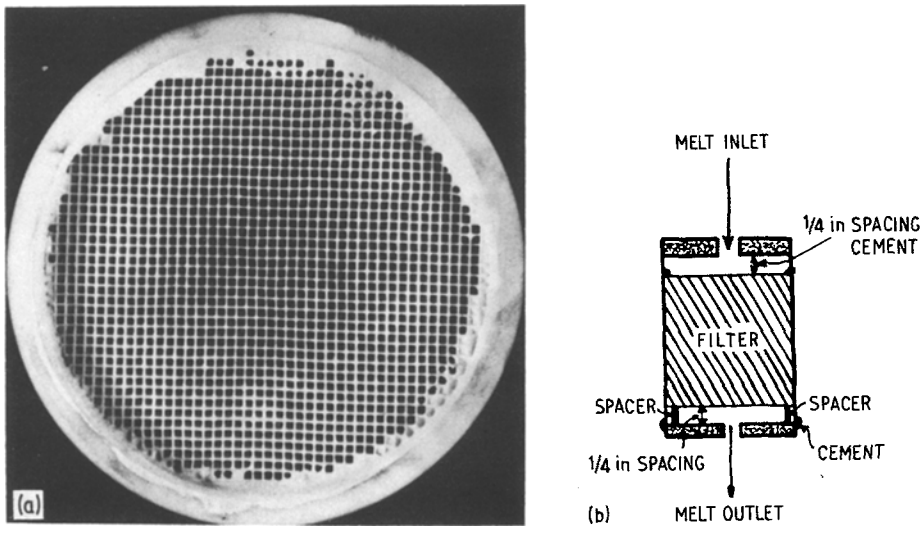

Figure 4 (a) Cemented monolithic alumina filter ready to use. (b) Schematic view of monolithic filter set-up.

TABLE I Inclusion size distribution in filtered and unfiltered steel

Inclusion size range (μm)	Number of inclusions per mm^2										
	Unfiltered melt	Filtered melt									
		Tabular filter*							Monolithic filter†		
		L = 5 cm			L = 10 cm		L = 15 cm			L = 5 cm	L = 10 cm
		U_i(cm sec^{-1})‡			U_i(cm sec^{-1})‡		U_i(cm sec^{-1})‡			U_i(cm sec^{-1})‡	U_i(cm sec^{-1})‡
		0.10	0.13	0.23	0.08	0.13	0.10	0.25	0.68	0.08	0.15	0.13
< 0.5	1976	1320	1000	988	26	70	212	160	300	243	582	162
0.5–1.0	1176	580	300	580	12	60	51	90	105	39	670	52
1.0–1.5	500	150	70	260	5	110	13	60	32	9	180	25
1.5–2.0	180	55	–	44	4	80	4	40	9	–	39	–
2.0–2.5	60	35	–	9	2	200	–	20	–	–	11	–
2.5–3.0	30	17	–	5	1	70	–	10	–	–	–	–
3.0–3.5	20	15	–	1	1	50	–	–	–	–	–	–
3.5–4.0	10	7	–	–	1	37	–	–	–	–	–	–
4.0–4.5	6	4	–	–	1	25	–	–	–	–	–	–
4.5–5.0	3	2	–	–	–	18	–	–	–	–	–	–

*0.2 to 0.5 cm nominal size.
†400 cells in^{-2}.
‡U_i is the melt interstitial velocity which is equivalent to U_m/ε, where U_m is superficial velocity (volumetric flow rate/cross-sectional area, cm^{3}sec^{-1}cm^{-2}) and ε is the bed porosity. ε for tabular filters is 0.40 and for monolithic filters is 0.63.

measured at several points with W–5%Re and W–26%Re thermocouples. Before the charge is heated, top and bottom chambers were evacuated and backfilled with argon up to a pressure of 1 atm. Argon was continuously circulated during heating of the charge. Once the charge was melted, it was held at 1600 ± 10°C for 30 min, a sample from the centre of the melt was sucked into a silica tube. High purity aluminium wire was then added to deoxidize the melt. About 3 min after the aluminium addition to the melt, a second sample from the centre of the melt was taken. The system now being ready for filtration, the top chamber was pressurized with argon and the stopper rod was raised, permitting the melt to flow through the filter.

The independent variables considered are: concentration of inclusions in the unfiltered melt, filter height and melt velocity. The dependent variable being the inclusion concentration of the filtered metal. All filtered and non-filtered samples were analysed via quantitative metallography using the TAS unit. Inclusion removal efficiency based on number, volume and weight of inclusions in the filtered (F) and non-filtered (NF) steel melts were calculated from the quantitative metallography data. The efficiency terms used are defined as:

$$\eta_N, \text{ number efficiency} = \frac{(\text{no. of inclusions})_{NF} - (\text{no. of inclusions})_F}{(\text{no. of inclusions})_{NF}}$$

$$\eta_V, \text{ volume efficiency} = \frac{(\text{total volume of inclusions})_{NF} - (\text{total volume of inclusions})_F}{(\text{total volume of inclusions})_{NF}}$$

In addition, all filtered and non-filtered samples were analysed chemically for soluble aluminium, insoluble aluminium, total aluminium and total oxygen. Weight per cent efficiency was calculated as follows:

$$\eta_W, \text{ weight efficiency} = \frac{(\text{total oxygen content, wt \%})_{NF} - (\text{total oxygen content, wt \%})_F}{(\text{total oxygen content, wt \%})_{NF}}$$

4. Results

Both types of filter which were used in this investigation showed no physical evidence of erosion or mechanical spalling. The filters maintained physical integrity at steel filtration temperatures.

The data from the TAS quantitative metallo-

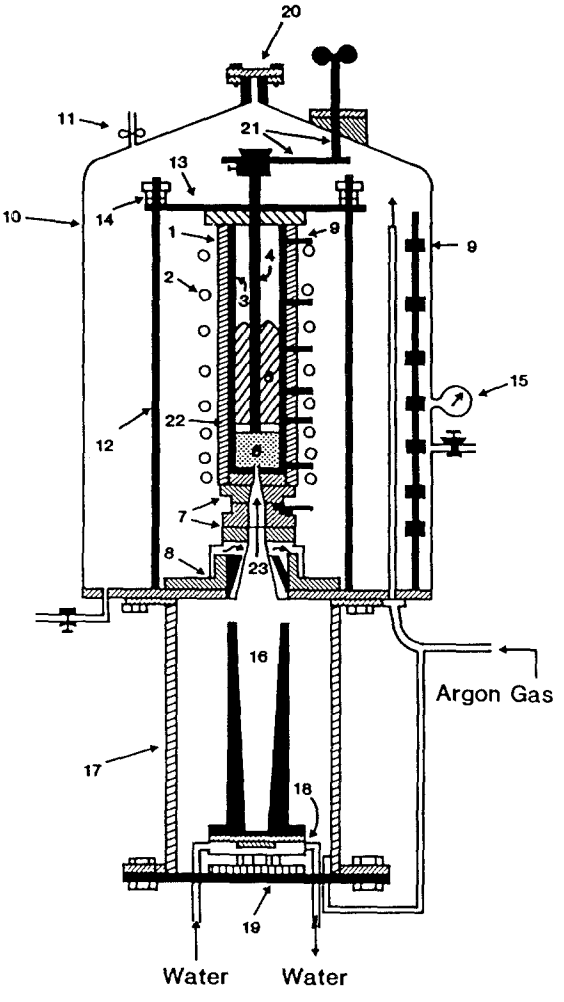

Figure 5 Schematic diagram of steel melt filtration apparatus. 1, Graphite susceptor; 2, induction coil; 3, alumina crucible; 4, alumina stopper rod; 5, steel melt; 6, alumina filter bed; 7, pyrolitic graphite rings; 8, water-cooled stainless steel pedestal; 9, thermocouples (W–5Re, W–26Re); 10, furnace dome; 11, safety valve; 12, steel rod; 13, steel plate; 14, springs; 15, pressure gauge; 16, metallic mould; 17, lower chamber; 18, water-cooled brass plate; 19, load cell; 20, opening window; 21, steel rod; 22, alumina disc; 23, orifice.

graphy for different heights of the tabular and monolithic filters are given in Table I. The number of inclusions observed per mm^2 of the sample in a given inclusion size range such as 0.5 to 1 μm, to 1 to 1.5 μm, etc. are given in Table I. A large reduction in inclusion concentrations can be noted between the filtered and unfiltered samples. From the TAS data, filter performance based on inclusion volume efficiency (η_V) and number efficiency (η_N) are given in Tables II and III, respectively. The calculated values in Tables II and III indicate that inclusions larger than 2.5 μm were completely removed by filtration.

Fig. 6 shows the comparison of inclusion size distribution data for unfiltered and filtered steel using 15 cm long tabular alumina filter at two different melt velocities, 0.10 and 0.68 cm sec^{-1}. The melt filtered at lower melt velocity contains fewer inclusions as compared to the melt filtered at a higher velocity. Fig. 7 shows the comparison of inclusion size distribution data for unfiltered and filtered steel using 5 cm long monolithic alumina filter at melt velocities of 0.08 and 0.15 cm sec^{-1}. It can be noted that a significant fraction of inclusions of submicron size can be removed from the steel melt and inclusions larger than 3 μm in size are completely removed. The inclusion size distribution data for unfiltered and filtered steel using 5 and 10 cm long monolithic alumina filters at a melt velocity of 0.13 to 0.15 cm sec^{-1} are shown in Fig. 8. These results indicate that for a given melt velocity, inclusion removal efficiency increases with increasing filter length.

A comparison of the filter performance for both tabular and monolithic filters is shown graphically in Fig. 9 with filter height and melt velocity being equal. These results show that there is no significant difference between the filters evaluated in terms of inclusion removal. An important observation, however, is that ~ 60 to 70% of the inclusions smaller than 0.5 μm can be removed by both tabular and monolithic filters.

5. Discussion

Number efficiencies, η_N, of inclusion removal as a function of size range for the 5 cm and 15 cm long tabular filters in the melt velocity range of 0.1 to 0.68 cm sec^{-1} are shown in Fig. 10. The volume efficiencies of these filters are given in Fig. 11. The effect of the melt velocity is evident; at lower melt velocities 0.10 cm sec^{-1}, higher inclusion removal efficiencies are obtained in contrast to the data from much higher melt velocities, 0.68 cm sec^{-1}. Lower melt velocities result in longer melt residence times in the filter than at higher melt velocities. The longer time the inclusions spend in the filter, the higher is the probability of their transport and subsequent sintering to the filter surface. At higher melt velocities, the smaller inclusions (< 0.5 μm) do not leave the melt stream-lines and thus are not

TABLE II Filtration performance based on volume of inclusions

Inclusion size range (μm)	Volume efficiency, η_V(%)										
	Tabular filter*								Monolithic filter†		
	L = 5 cm			L = 10 cm		L = 15 cm			L = 5 cm		L = 10 cm
	U_i(cm sec^{-1})‡			U_i(cm sec^{-1})‡		U_i(cm sec^{-1})‡			U_i(cm sec^{-1})‡		U_i(cm sec^{-1})‡
	0.10	0.13	0.23	0.08	0.13	0.10	0.25	0.68	0.08	0.15	0.13
< 0.5	5.7	64.1	56.1	98.1	92.5	86.0	88.7	66.0	88.7	60.4	94.3
0.5–1.0	33.3	67.8	14.4	98.9	87.8	91.7	93.3	83.3	95.6	40.0	93.3
1.0–1.5	50.0	93.8	–	100	61.3	92.5	78.8	93.8	98.8	48.8	92.5
1.5–2.0	57.8	100	80.7	98.3	27.7	100	72.3	100	100	80.7	100
2.0–2.5	41.5	100	94.3	100	–	100	84.9	100	100	100	100
2.5–3.0	51.2	100	100	92.2	75.6	100	100	100	100	100	100
3.0–3.5	10.0	100	75.0	100	–	100	100	100	100	100	100
3.5–4.0	0.0	100	100	100	–	100	100	100	100	100	100
4.0–4.5	33.3	100	100	–	–	100	–	100	100	100	100
4.5–5.0	–	100	100	100	100	100	100	100	100	100	100

*0.2 to 0.5 cm nominal size.
†400 cells in^{-2}.
‡U_i is the melt interstitial velocity which is equivalent to U_m/ε, where U_m is superficial velocity (volumetric flow rate/cross-sectional area, cm^3 sec^{-1} cm^{-2}) and ε is the bed porosity. ε for tabular filters is 0.40 and for monolithic filters is 0.63.

captured as readily as the larger inclusions (> 1.5 μm). Similar trends are observed for the 5 cm long monolithic extruded alumina filters which were used at 0.08 and 0.15 cm sec^{-1} melt velocities – see Fig. 12. As in the tabular filters evaluated, at the low melt velocities (0.08 to 0.10 cm sec^{-1}) 100% removal efficiencies were obtained for inclusions larger than 1.5 μm. The length of the filter used has a considerable effect on inclusion removal. This is graphically shown

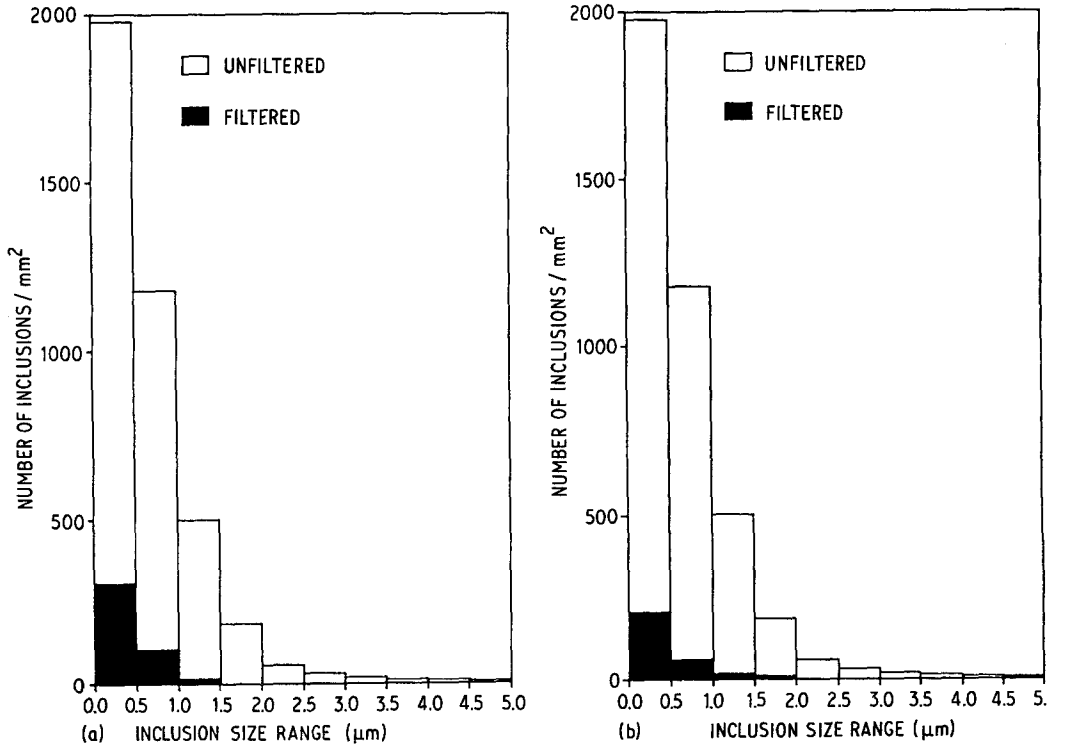

Figure 6 Effect of melt interstitial velocity on filtration performance for 15 cm long tabular alumina filters. (a) U_i = 0.68 cm sec^{-1}, (b) U_i = 0.10 cm sec^{-1}.

TABLE III Filtration performance based on number of inclusions

Inclusion size range (μm)	Volume efficiency, η_N(%)										
	Tabular filter*								Monolithic filter†		
	L = 5 cm			L = 10 cm		L = 15 cm			L = 5 cm		L = 10 cm
	U_i(cm sec^{-1})‡			U_i(cm sec^{-1})‡		U_i(cm sec^{-1})‡			U_i(cm sec^{-1})‡		U_i(cm sec^{-1})‡
	0.10	0.13	0.23	0.08	0.13	0.10	0.25	0.68	0.08	0.15	0.13
< 0.5	33.2	49.4	50.0	98.7	96.5	89.3	91.9	84.8	87.7	70.6	91.8
0.5–1.0	50.7	71.9	50.7	98.9	94.9	95.7	92.3	91.1	96.7	43.0	95.8
1.0–1.5	70.0	85.9	48.0	99.0	78.0	97.4	88.0	93.6	98.4	64.0	95.0
1.5–2.0	69.4	100	75.6	97.8	55.6	97.8	77.8	95.0	100	78.3	100
2.0–2.5	41.7	100	85.0	96.7	–	100	66.7	100	100	81.7	100
2.5–3.0	43.3	100	83.3	96.7	–	100	66.7	100	100	100	100
3.0–3.5	25.0	100	95.0	95.0	–	100	100	100	100	100	100
3.5–4.0	30.0	100	100	90.0	–	100	100	100	100	100	100
4.0–4.5	33.3	100	100	83.0	–	100	100	100	100	100	100
4.5–5.0	33.3	100	100	100	–	100	100	100	100	100	100

*0.2 to 0.5 cm nominal size.
†400 cells in^{-2}.
‡U_i is the melt interstitial velocity which is equivalent to U_m/ε, where U_m is superficial velocity (volumetric flow rate/cross-sectional area, cm^3 sec^{-1} cm^{-2}) and ε is the bed porosity. ε for tabular filters is 0.40 and for monolithic filters is 0.63.

in Fig. 13 which illustrates the data for monolithic extruded filters tested at 0.13 and 0.15 cm sec^{-1} melt velocities; doubling the height of the monolithic filter, from 5 to 10 cm, increases the filtration performance by 20% (for the longer inclusions – > 1.5 μm) and to 75 to 80% (for the small inclusions – 0.5 to 1.0 μm).

The filtration performance of both the tabular and monolithic ceramic filters are comparable as can be noted in Fig. 14. The results agree with and confirm the filtration efficiency expression [10] based on a mathematical model of liquid metal filtration,

$$\eta = \frac{C_i - C_0}{C_i} = 1 - \frac{C_0}{C_i} \qquad (1)$$

where: η is the inclusion removal efficiency, C_i the concentration of inclusions in the melt at the inlet to the filter, and C_0 the concentration of inclusions in the melt at the outlet to the filter. C_0

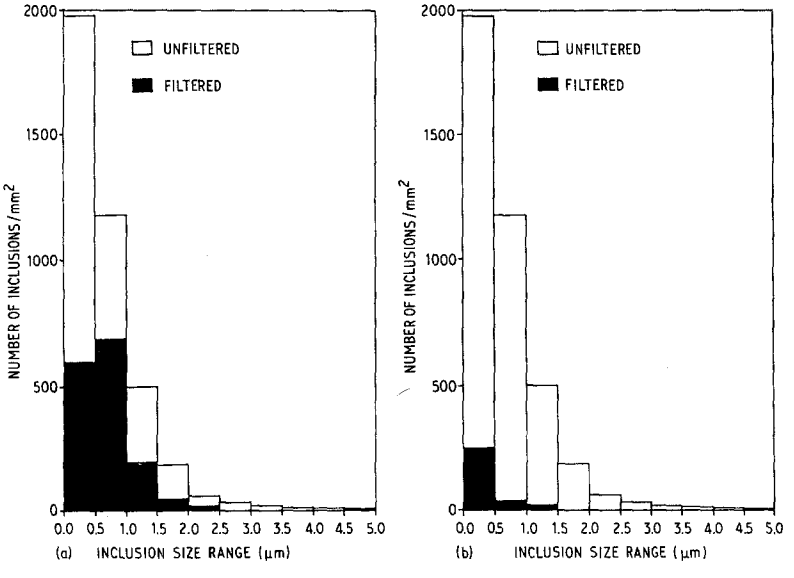

Figure 7 Effect of melt interstitial velocity on filtration performance for 5 cm long monolithic alumina filters. (a) U_i = 0.15 cm sec^{-1}, (b) U_i = 0.08 cm sec^{-1}.

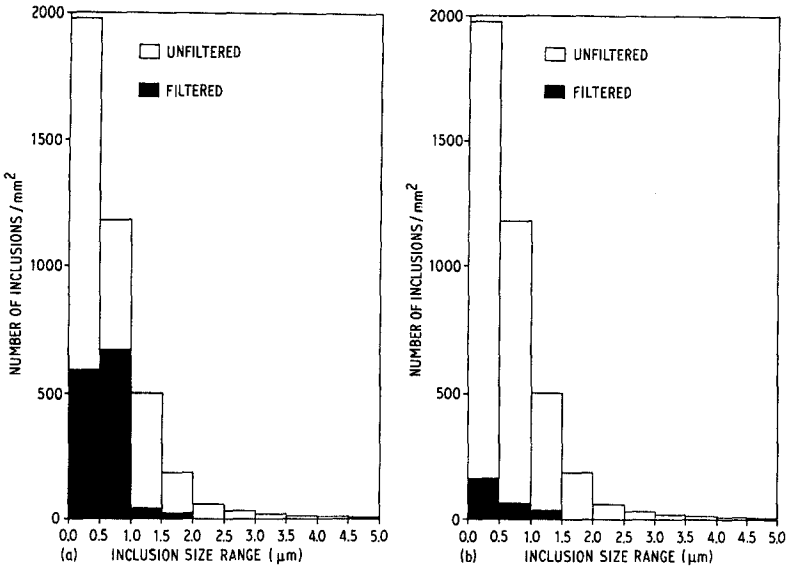

Figure 8 Effect of monolithic filter length on filtration performance. Filter length = 5 cm. (a) $U_i = 0.15$ cm sec^{-1}, (b) $U_i = 0.13$ cm sec^{-1}.

is expressed as follows:

$$C_0 = C_i \exp\left(-\frac{K_0 L}{U_m}\right) \quad (2)$$

where K_0 is the kinetic parameter, L the filter length, and U_m the superficial melt velocity.

Substituting the above in Equation 1, one obtains:

$$\eta = 1 - \exp\left(-\frac{K_0 L}{U_m}\right) \quad (3)$$

It can be seen from Equation 3 that removal efficiency increases with decreasing melt velocity (U_m) and increasing filter length (L). This agrees with the observed results shown in Figs. 6 to 9 and 10 to 13. The filter surface characteristics were evaluated using scanning electron microscopy (SEM). Fig. 15 shows the surface topography of the tabular and monolithic filters. It can be noted that the surface of the tabular filter is smoother than that of the monolithic filter. The total surface area of the filter bed which is

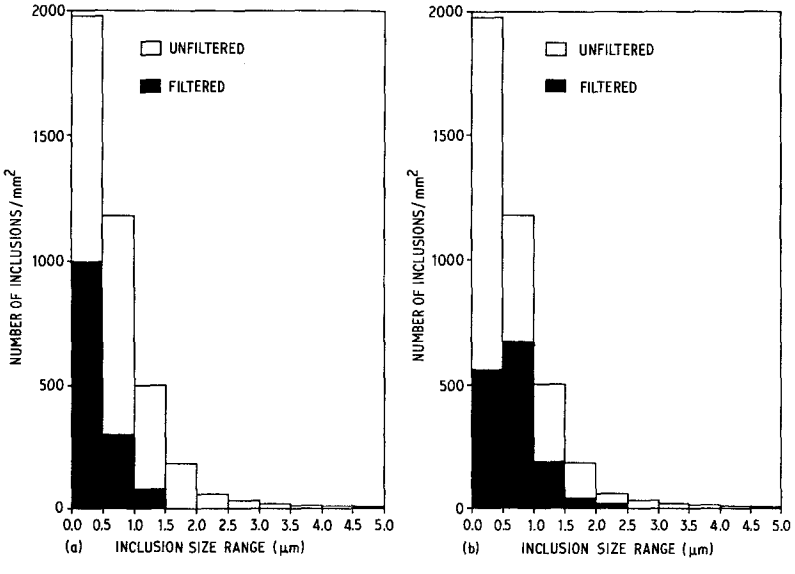

Figure 9 Effect of filter morphology and characteristics on filtration performance for 5 cm filter length. (a) $U_i = 0.13$ cm sec^{-1}, (b) $U_i = 0.15$ cm sec^{-1}.

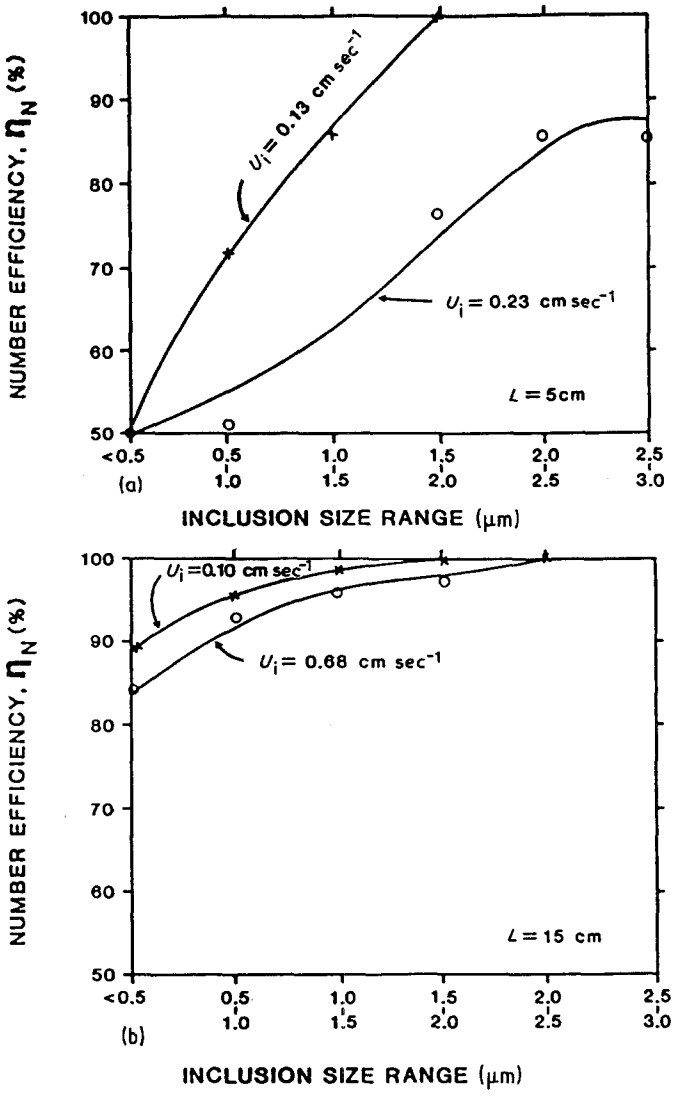

Figure 10 Effect of melt interstitial velocity on number efficiency for tabular alumina filters: (a) 5 cm long filter; (b) 15 cm long filter.

exposed to the molten metal directly influences inclusion capture. For a given filter volume, the monolithic extruded filter has a larger surface area exposed to the melt than the tabular filter.

Inclusion attachment to the filter surface takes place all along the length of the filter; however, a large fraction of the inclusions are captured in the upper section of the filter (at the entry) and the fraction captured decreases as one travels down the filter towards the exit point. Fig. 16 shows the inclusion attachment in a spent tabular filter. The spent filter beds were etched with bromine-methanol and inclusion attachments to the filter particle surface were examined. Fig. 17 shows attached and captured inclusions at the surface of a monolithic filter. The results show that a large number of inclusions are deposited in the entry part of the filter.

Extensive chemical analyses of filtered and unfiltered samples were carried out for total oxygen content (O_T) and are reported elsewhere [8]. It is interesting to compare the filter performance results based on total oxygen analysis to those evaluated by quantitative metallography. In Fig. 18 removal efficiencies determined by the two techniques are presented along with the 100% correlation line. The data given in Fig. 18 clearly show a strong correlation between the two methods of analysis.

6. Conclusions

1. It has been shown that the number of

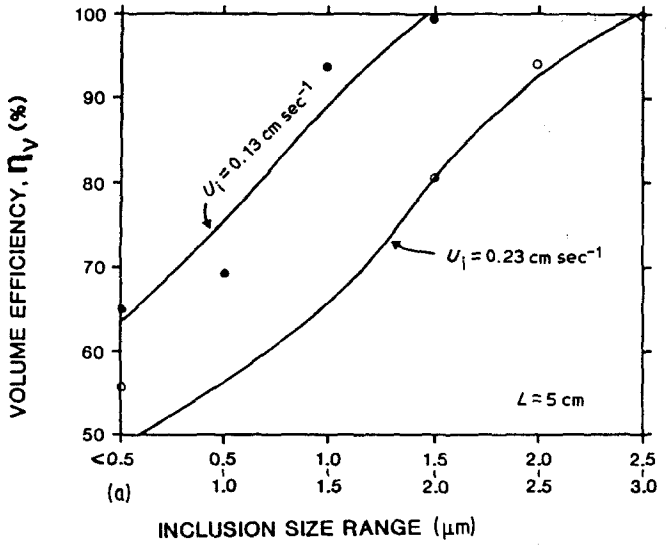

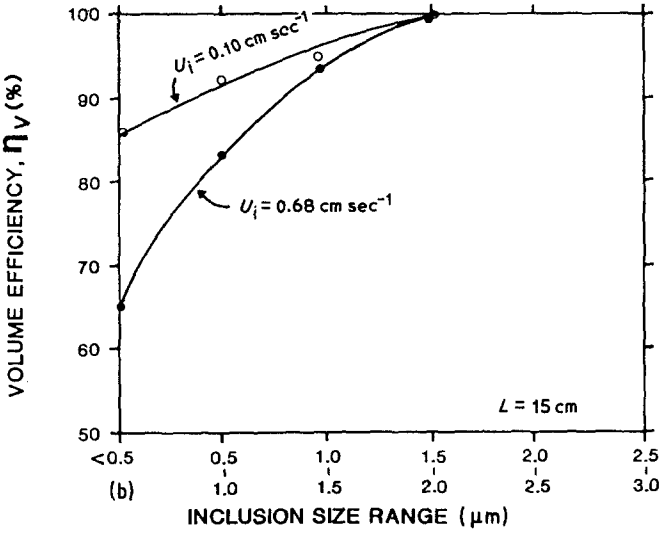

Figure 11 Effect of melt interstitial velocity on volume efficiency for tabular alumina filters: (a) 5 cm long filter; (b) 15 cm long filter.

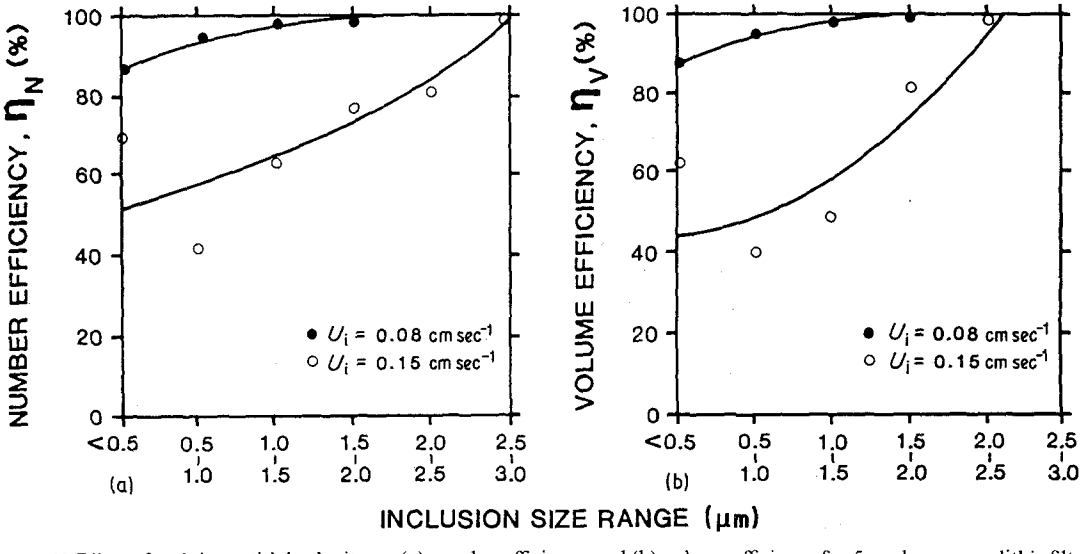

Figure 12 Effect of melt interstitial velocity on (a) number efficiency and (b) volume efficiency for 5 cm long monolithic filters.

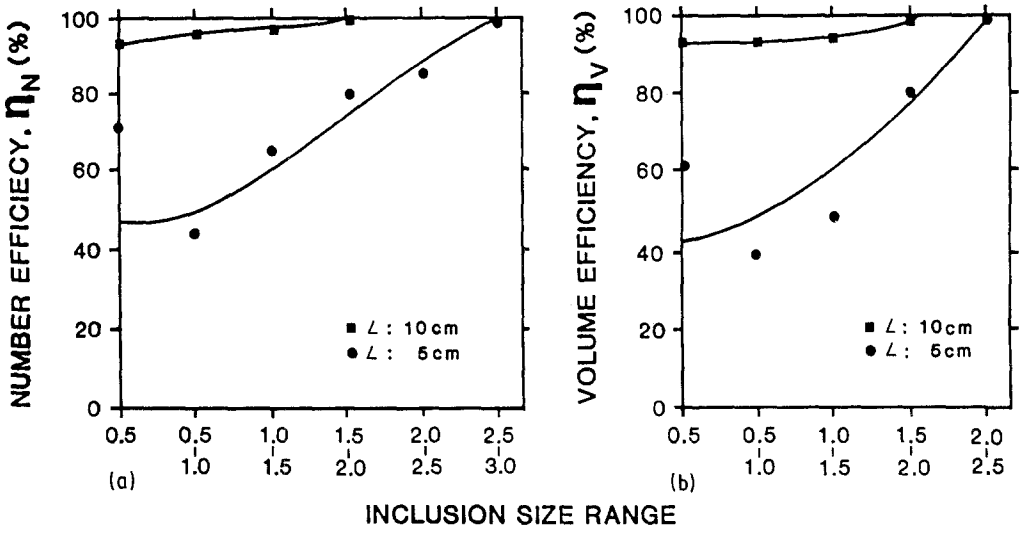

Figure 13 Effect of monolithic filter length on (a) number efficiency and (b) volume efficiency for a melt interstitial velocity in the range 0.13 to 0.15 cm sec^{-1}.

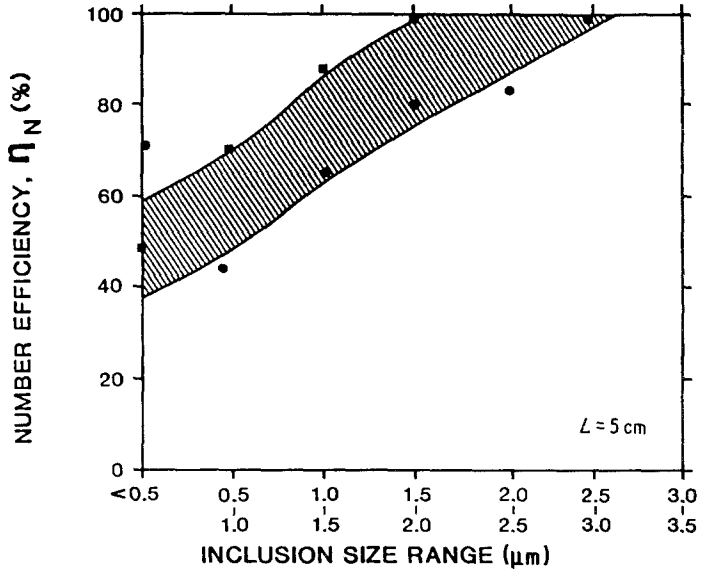

Figure 14 Effect of filter morphology on number efficiency for 5 cm long filter in the melt velocity range 0.13 to 0.15 cm sec^{-1}. ■ tabular, ● monolithic.

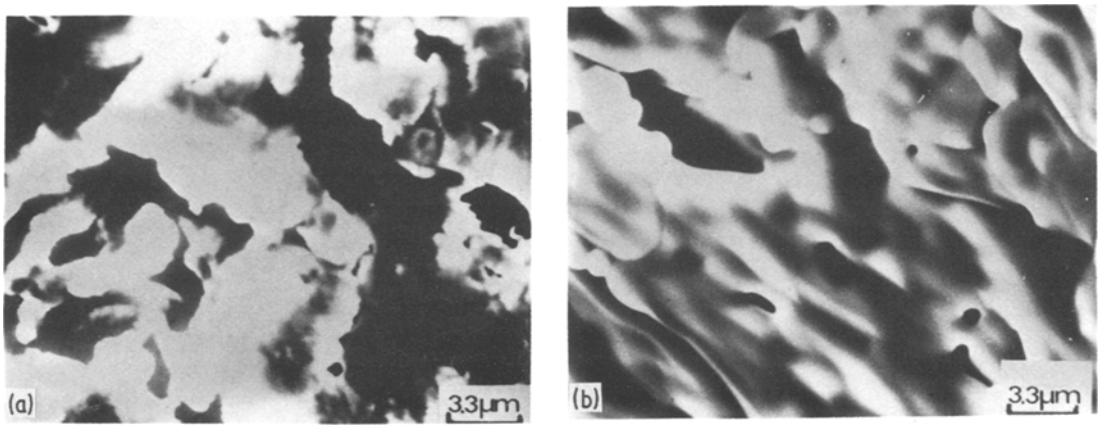

Figure 15 (a) Scanning electron micrograph showing the surface topography of the (a) tabular monolithic alumina particle, and (b) the monolithic alumina filter.

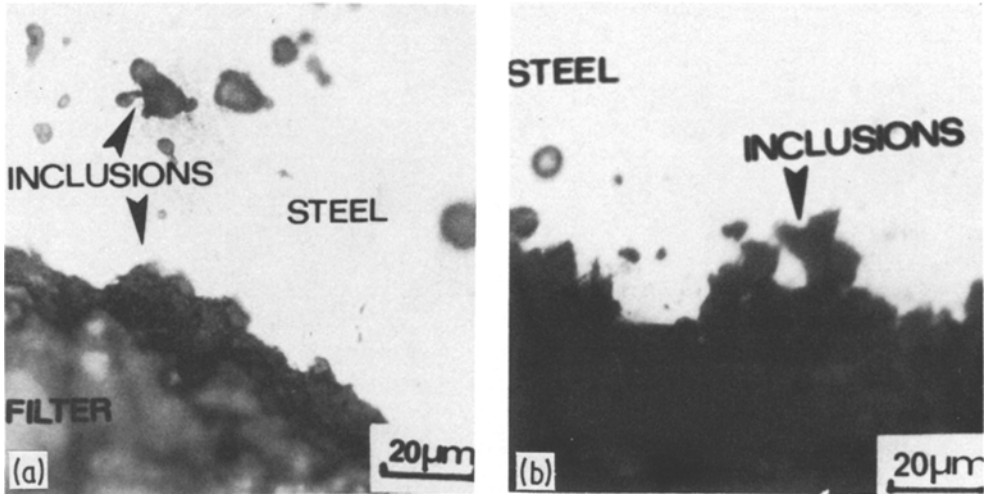

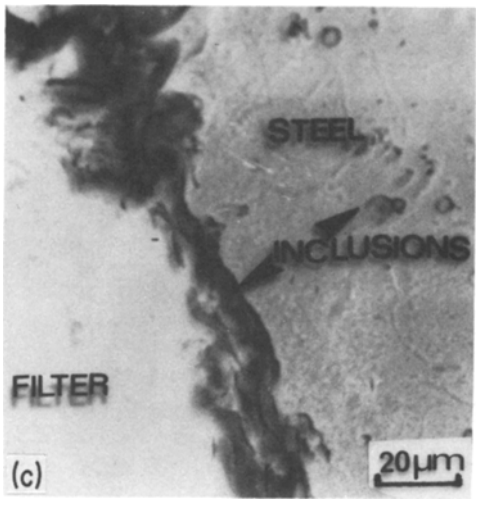

Figure 16 Photomicrographs showing the presence of inclusions in the used tabular alumina filter volume. (a) and (b) Optical micrographs of the top and bottom portions, respectively, of the filter. (c) Scanning electron micrograph showing the inclusion attachment to the filter grain (sample etched with bromine-methanol).

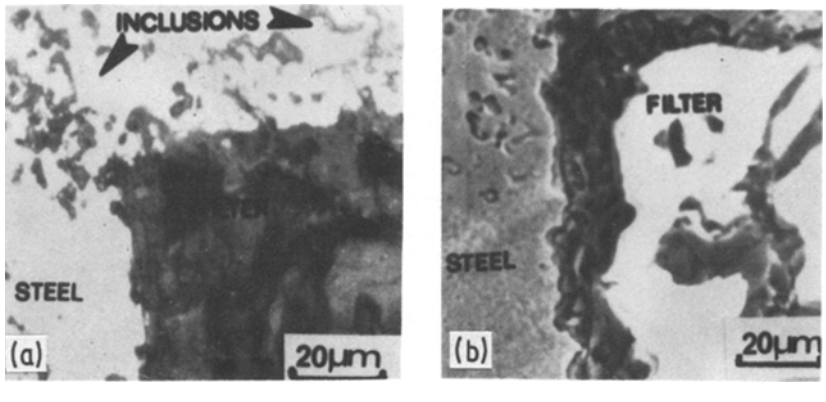

Figure 17 Photomicrographs showing the presence of inclusions in the used monolithic filter volume. (a) Optical micrograph of the entrance to the filter; (b) scanning electron micrograph of the entrance to the filter; (c) and (d) optical micrographs of the middle and bottom parts, respectively, of the filter.

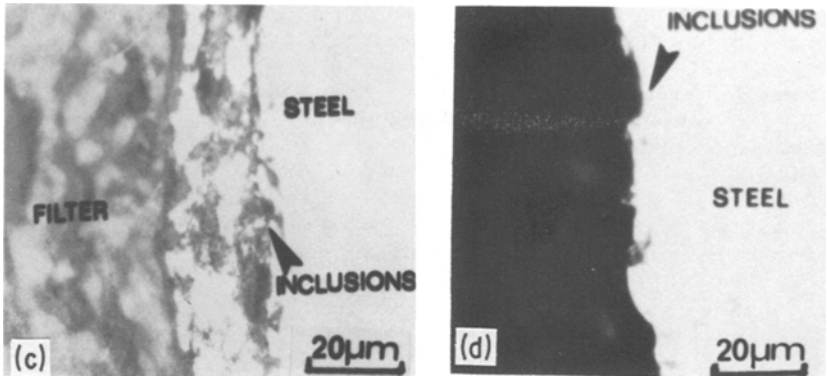

Figure 17 Continued.

inclusions have been substantially reduced in molten steel by filtering the melt through alumina based ceramic media, monolithic extruded and tabular granules.

2. Inclusion removal efficiencies ranged between 45 and 100% depending on (a) melt velocity through the filter; (b) height of the filter; and (c) inclusion size.

Increasing the melt velocity through the filter decreases the inclusion removal efficiency, which is due to the reduced melt residence time in the filter.

Increasing filter length increases the inclusion removal efficiency.

The quantitative metallographic results show that higher inclusion removal efficiencies were obtained for the larger size inclusions, 1.5 to 2.5 μm, than for the 0.5 to 1.0 μm size inclusions. Moreover, inclusions larger than 2.5 μm were completely removed by the two filters evaluated in this study.

Acknowledgements

The authors would like to acknowledge the AISI for support of this work and Dr Alan Cramb of Homer Research Laboratories, Bethlehem Steel Corporation, Dr Anil Lingras of Lukens Steel, and Dr Pete Koros of LTV Steel.

References

1. J. W. JUPPENLATZ and S. W. GEARHART, *Steel Foundry Facts* No. 331, (March 1979).
2. M. ATKINSON, *J. Iron Steel Inst.* **165** (1960) 64.
3. H. N. CUMMING, F. B. STULEN and W. C. SCHULTE, *Proc. ASTM* **58** (1958) 505.

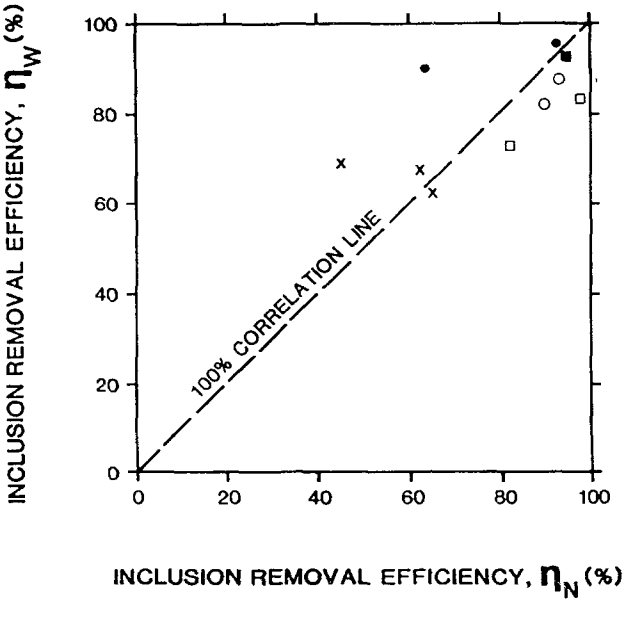

Figure 18 Comparison of inclusion removal efficiencies based on weight and number of inclusions using tabular and monolithic alumina filters. Tabular; L = (x) 5, (□) 10 and (○) 15 cm. Monolithic; L = (●) 5 and (■) 10 cm.

4. J. L. MIHELICH, J. R. BELL and M. J. KARCHYNSKY, *J. Iron Steel Inst.* **209** (1971) 469.
5. Scaninject I, Proceedings of International Conference on Ladle Refining and Injection Metallurgy, Lulea, Sweden, June 1977 (Jernkontoret, Sweden).
6. Scaninject II, Proceedings of International Conference on Ladle Refining and Injection Metallurgy, held in Lulea, Sweden, June 1980 (Jernkontoret, Sweden).
7. Scaninject III, Proceedings of International Conference on Ladle Refining and Injection Metallurgy, held in Lulea, Sweden, June 1983 (Jernkontoret, Sweden).
8. S. ALI, PhD thesis, Drexel University (1984).
9. L. A. SPEILMAN, *Ann. Rev. Fluid Mech.* **9** (1977) 297.
10. D. APELIAN and R. MUTHARASAN, *J. Metals* **32**, September (1980) 14.

Received 18 September
and accepted 15 October 1984